J. of Supercritical Fluids 67 (2012) 114–122

Contents lists available at SciVerse ScienceDirect

The Journal of Supercritical Fluids

journal homepage: www.elsevier.com/locate/supflu

Architecture and properties of bi-modal porous scaffolds for bone regeneration prepared *via* supercritical CO_2 foaming and porogen leaching combined process

A. Salerno[a,b,*], S. Zeppetelli[b], E. Di Maio[c], S. Iannace[b], P.A. Netti[a,c]

[a] Center for Advanced Biomaterials for Health Care, Istituto Italiano di Tecnologia (IIT@CRIB), Largo Barsanti e Matteucci, 80125 Naples, Italy
[b] Institute of Composite and Biomedical Materials, National Research Council (IMCB-CNR), Piazz.le Tecchio 80, 80125 Naples, Italy
[c] Department of Materials and Production Engineering (DIMP), University of Naples Federico II, Piazz.le Tecchio 80, 80125 Naples, Italy

ARTICLE INFO

Article history:
Received 28 December 2011
Received in revised form 30 March 2012
Accepted 31 March 2012

Keywords:
Hydroxyapatite
Poly(ε-caprolactone)
Scaffold
Supercritical CO_2 foaming
Zein

ABSTRACT

The aim of this study was the design of bi-modal porous scaffolds for bone tissue engineering (bTE) by combining supercritical CO_2 ($scCO_2$) foaming and porogen leaching techniques.

Poly(ε-caprolactone) (PCL) was melt blended with thermoplastic zein (TZ) w/o the addition of 20 wt.% of HA particles to prepare a 40/60 (w/w) co-continuous blend and a 32/48/20 multi-phase composite, respectively. The materials were subsequently gas foamed by using $scCO_2$ as blowing agent. Saturation and foaming temperatures and pressures, as well as depressurization time were selected in order to optimize the pore structure of the foams and, to induce the formation of a macro-porosity suitable for bone cell adhesion and colonization. The foams were subsequently soaked in water in order to leach out the plasticizer from the TZ phase and, to induce the formation of a bi-modal pore structure.

The effect of the composition of the materials and the foaming parameters on the properties of the scaffolds was assessed by SEM, image analyses and static compression tests. Furthermore, *in vitro* cell cultures were performed by using MG63 osteoblasts to assess the biocompatibility of the scaffolds and, to evaluate their capacity to promote cell adhesion, colonization and proliferation.

The results of this study demonstrated that the proposed technique allowed for the design and fabrication of bi-modal porous PCL/TZ and PCL/TZ-HA composite scaffolds by a green process. In particular, the scaffolds showed a 20–400 μm macro-porosity, obtained by performing the $scCO_2$ foaming process at a temperature higher than PCL melting, coupled with a 3 μm micro-porosity, obtained by leaching out the plasticizer from the TZ phase. Finally, the biological characterization demonstrated that the scaffolds allowed cell adhesion, colonization and proliferation up to 28 days of *in vitro* culture, therefore demonstrating potential for bTE.

1. Introduction

In the past two decades, the repair and reconstruction of musculoskeletal tissues by using biodegradable scaffold materials has emerged as one of the most promising approaches in bone tissue engineering (bTE) [1,2]. In this approach, the biodegradable scaffold is designed appropriately to provide a temporary extracellular matrix analog for transplanted cells to attach, grow and maintain their differentiated functions *in vitro* and/or *in vivo* [1,2].

Among the wide range of properties of the scaffold that affect its biological performances, the micro-architecture of the pore-structure was found to be key determinant for the regeneration of a functional tissue [3,4]. For instance, in the case of bTE, there are several studies demonstrating that optimal pore sizes is about 5 μm to allow for construct vascularization and, in the range from 100 to 400 μm to permit cell and tissue ingrowths [1,3]. Moreover, it has been recently demonstrated that the new-bone regeneration may be improved when the scaffold is provided of a bi-modal pore size distribution with both pore size scales [4–6]. Indeed, the combination of the macro-porosity and micro-porosity networks may allow for the fabrication of a porous scaffold suitable for the three-dimensional colonization, proliferation and migration of cells, as well as for new-tissue vascularization and improved nutrients transport, protein adsorption and cell adhesion/biosynthesis [4–6].

There are several processing technologies that have been developed and implemented in tissue engineering to produce porous scaffolds, among them the selective extraction of soluble templates, thermodynamically based processes and bottom-up approaches are the most investigated [3–11]. Supercritical CO_2 ($scCO_2$) foaming has recently achieved great emphasis in TE because of the possibility to fabricate porous scaffolds avoiding the use of organic

* Corresponding author at: Center for Advanced Biomaterials for Health Care, Istituto Italiano di Tecnologia (IIT@CRIB), Largo Barsanti e Matteucci, 80125 Naples, Italy. Tel.: +39 0817682536.
E-mail address: asalerno@unina.it (A. Salerno).

0896-8446/$ – see front matter © 2012 Elsevier B.V. All rights reserved.
http://dx.doi.org/10.1016/j.supflu.2012.03.016

solvents that are potentially harmful to cells and biological tissues [8–10]. Furthermore, the rather low $scCO_2$ temperature (31.1 °C) and pressure (7.4 MPa), may also offer the possibility of simultaneously processing biomaterials, growth factors and cells at ambient temperature, allowing for the production of drug releasing scaffolds as well as cell/scaffold constructs in a single step [9,10]. Another important advantage of this technique is the chance of fine tuning the architecture of the pore structure of the scaffolds through proper selection of the processing conditions, mainly solubilization pressure (gas concentration), foaming temperature and depressurization time [8,11].

Several biocompatible and biodegradable polymers, from both natural and synthetic origin, were proposed for repairing bone defects. Among synthetic polymers, poly(ε-caprolactone) (PCL) is now regarded as a bone tissue compatible material due to its ability to support the *in vitro* and *in vivo* bone cell/tissue growth for several months, without inducing a toxic response and, preserving its mechanical function [1,3,6]. Furthermore, we have recently shown that multi-phase biomaterials obtained by blending PCL with thermoplastic zein (TZ), a thermoplastic polymer prepared by mixing zein with poly(ethylene glycol) (PEG) 400, under particular heat and shear conditions, and hydroxyapatite (HA) particles improved the *in vitro* differentiation of mesenchymal stem cells and MG63 osteoblasts if compared to neat PCL [12,13]. These results were in agreement with those of other works that reported the ability of zein, a major storage protein of corn, and HA, one of the main component of the inorganic matrix of bone, to promote cell adhesion, proliferation and osteogenic differentiation *in vitro*, and new-bone regeneration when implanted *in vivo* [14–18].

Along with this research line, in this work we combined $scCO_2$ foaming and porogen leaching techniques aiming to fabricate bi-modal porous PCL/TZ and PCL/TZ-HA scaffolds for bTE. In particular, the foaming process was optimized in order to create a macro-porosity network within the PCL phase. Furthermore, the foamed samples were soaked in water at 37 °C overnight to leach out the plasticizer from the TZ phase and, to induce the formation of an additional micro-porosity pattern within the samples.

The as obtained scaffolds were characterized by scanning electron microscopy, Image analysis and static compression tests to assess their morphology, pore structure and mechanical properties, respectively. Finally, *in vitro* biological tests were performed up to 28 days to evaluate the biocompatibility of the scaffolds and to demonstrate their potential for bTE.

2. Materials and methods

2.1. Materials

PCL (M_W = 65 kDa) and maize zein powder (Z3625, batch: 065K0110) were purchased from Sigma–Aldrich (Milan, Italy). PEG 400 was purchased from Fluka (Milan, Italy) and used as plasticizer for the preparation of the TZ. Micrometric HA particles (70–105 μm size, Fin-Granule) were kindly supplied by Finceramica (Faenza, Italy).

2.2. Multi-phase biomaterial's preparation

The TZ was prepared by melt mixing zein powder with 25 wt.% of PEG 400 in a twin counter rotating internal mixer (Rheomix 600, Haake, Karlshrue, Germany) controlled by a measuring drive unit (Rheocord 9000 Haake, Germany) at 80 °C, 50 rpm and 10 min.

The same mixing equipment was used for the preparation of multi-phase biomaterials. In particular, PCL pellets were first melted at 70 °C, 20 rpm for 2 min and, subsequently, TZ and HA granules were added into the mixing chamber and mixed at 70 °C, 80 rpm for 6 min. The compositions were: 40/60 (w/w) for the PCL/TZ blend and 32/48/20 (w/w/w) for the PCL/TZ-HA composite. Finally, the compounds were compression molded at 80 °C and 30 MPa into 2 mm-thick plates by a hot press (P300P, Collin, Ebersberg, Germany).

2.3. Scaffolds production via $scCO_2$ foaming and PEG leaching

The fabrication of the scaffolds was performed by combining the techniques of $scCO_2$ foaming and PEG leaching. In particular, the foaming process was optimized in order to create a macro-porosity network within the PCL phase, while the further leaching of the plasticizer from the TZ phase was performed to create a micro-porosity pathway.

Foaming experiments were carried out by placing disc-shaped samples (d = 10 mm and h = 2 mm) in a high pressure autoclave. Two different sets of experiments were performed to control the pore structure of the foamed samples.

In the first set of experiments, the autoclave was heated to 35 °C and, the CO_2 pressure increased to 20 MPa, therefore ensuring the achievement of the supercritical state. After 15 h of solubilization, foaming was induced by quenching the pressure to the ambient and selecting a low (15 s) or a high (120 s) depressurization time.

In the second set of experiments, the samples were solubilized at 9 MPa and 80 °C for 4 h, to ensure the complete PCL melting. The autoclave was then heated up to 110 °C and the pressure quenched to the ambient by a low depressurization time (15 s) to induce sample foaming. To stabilize the pore structure, foams were immediately cooled down to ambient temperature. This was achieved with the aid of a heat exchanger equipped with a water/antifreeze solution as cooling bath and settled to the temperature of 0 °C. After cooling to the ambient, the samples were removed from the autoclave for further processes.

The final bi-modal scaffold pore structure was achieved by soaking selected foams in distilled H_2O at 37 °C, overnight. This additional process promoted the leaching of the PEG from the TZ phase and, induced the formation of an open micro-porosity network within the scaffolds.

2.4. Scaffolds characterization

The morphology, porosity and pore size distribution of the scaffolds were evaluated by scanning electron microscopy (SEM) (S440, Wetzler, LEICA) and image (Image J) analyses [6]. The scaffolds were cross sectioned, gold sputtered, and analyzed at an accelerating voltage of 20 kV. The SEM micrographs were converted first to binary images and, further analyzed by the Image J software to evaluate the porosity, the pore size distribution and the mean pore size of the scaffolds (ASTM D3576).

The static compression properties of the scaffolds were determined using an Instron mechanical testing system (4204, Instron, Milan, Italy), working at a cross head of 1 mm/min and, with a 1 kN loading cell. Five disc-shaped scaffolds (d = h = 5 mm) were tested for each type to determine the elastic compression modulus (E), evaluated as the slope of the initial linear portion of the stress (σ) *vs.* strain (ε) curve and, the compression yield strength (σ_Y) and strain (ε_Y), calculated with the modulus slope at 1% strain offset.

Human osteoblast MG-63 cells, kindly provided by Prof. Rodolfo Quarto, University of Genoa, Italy, were used to assess the *in vitro* biological response of the scaffolds. Cells were first cultured in 75-cm^2 flask at 37 °C and 5% CO_2, washed with PBS (Sigma–Aldrich, Italy) and incubated with trypsin–EDTA (0,25% trypsin, 1 mM EDTA, Euroclone, Italy) for 5 min at 37 °C.

Disk-shaped scaffolds (d = h = 5 mm) were γ-sterilized, pre-wetted with the medium for 2 h, statically seeded with 5×10^3 cells/scaffold and, re-suspended in 50 μL of medium. The

scaffolds were then placed in 24-well culture plates (1 scaffold/well), following incubation for 2 h to allow for cell adhesion. Subsequently, cell culture medium was added to each well to bring the total well volume to 1.5 mL. Culture medium used was Dulbecco's modified Eagle's medium supplemented with 10% fetal calf serum (Gibco-BRL Life Technologies, Milan, Italy) and antibiotics (penicillin G sodium 100 U/mL, streptomycin 100 μg/mL, Euroclone, Milan, Italy).

Cell viability and proliferation were evaluated by using Alamar Blue assay. At pre-determined time points, the cell/scaffold constructs were removed from the culture plates, washed with PBS and placed into 24-well culture plates. Then, 2 mL of DMEM medium without Phenol red (HyClone, UK) containing 10% (v/v) Alamar Blue (AbD Serotec Ltd., UK) were added to each well, and the constructs incubated for 4 h at 37 °C and 5% CO_2. The solution was subsequently collected and analyzed by a spectrophotometer (multilabel counter, 1420 Victor, Perkin Elmer, Italy) at the wavelengths of 570 and 600 nm. The number of viable cells per scaffold was assessed by comparing the absorbance values with those of the calibration curve. The calibration curve was obtained by the correlation between known cell numbers into the 24-well culture plates with the correspondent absorbance value. Five scaffolds for each composition were used.

Cell adhesion, morphology and colonization were investigated by SEM analysis. The cell/scaffold constructs were extracted from the wells, washed with PBS and fixed with 2.5% glutaraldehyde (Sigma–Aldrich, Italy) in 0.1 M Na-cacodylate (Carlo Erba, Italy) at pH 7.4. Before SEM examination, the constructs were freeze-dried overnight

2.5. Statistical analysis

The statistical significance of the results was assessed by one-way ANOVA. Tukey *post hoc* test at the significance level $p < 0.05$ was used to identify statistically different groups by using Origin® software package.

3. Results and discussion

To date, advances in bTE revealed that scaffolds characterized by bi-modal porous architecture are very promising for the regeneration of bone [4–6,8]. Based on these results, in this work we combined the techniques of $scCO_2$ foaming and porogen leaching for the design and fabrication of bi-modal PCL/TZ and PCL/TZ-HA porous scaffolds for bTE. In particular, the first part of this study focused on the foaming process of the prepared multi-phase materials, with the aim of producing porous foams with a macroporosity of the order of hundreds of microns and, consequently, suitable for bone cell adhesion, colonization and proliferation. Furthermore, the most interesting foams were selected in order to perform the leaching of the plasticizer from the TZ phase and, to fabricate bi-modal porous scaffolds for bTE. The second and third parts of this study were finally devoted to the characterization of the micro-structural and biological properties of the scaffolds, respectively.

3.1. $scCO_2$ foaming of PCL/TZ and PCL/TZ-HA samples and selective PEG extraction

The ability of $scCO_2$ to plasticize and in such cases dissolve polymeric biodegradable scaffold materials, such as PCL, at relatively low temperature, have recently opened new routes for the design and fabrication of porous scaffolds by the so called "solid-state $scCO_2$ foaming" [8,10,11]. Indeed, the solubilization of small amounts of $scCO_2$ within a polymer can result in a substantial and dramatic change in its physical properties, including viscosity and interfacial tension, as well as the decrease of its glass and melting temperatures down to the ambient temperature [19,20]. As a direct consequence, foaming may be possible at relatively "mild" conditions, allowing for the fabrication of porous scaffolds with controlled pore structures and pre-incorporated cells and/or bioactive factors [9,10]. However, the processing of biocompatible and biodegradable polymers *via* the solid-state $scCO_2$ foaming requires a careful control of the parameters involved in the blowing agent solubilization and foaming, such as solubilization pressure and time. Nevertheless, to achieve a fine control of scaffold microstructure it is also strongly required the optimization of material composition, molecular weight and cristallinity [6,8,11].

In the first part of this study we investigated the solid-state foaming of the multi-phase biomaterials prepared, with the ultimate goal of designing 3D porous scaffolds with micro-structural properties suitable for bTE.

In Fig. 1 the SEM micrographs of the cross-section of the resulting scaffolds are reported, clearly evidencing the heterogeneous distribution of the size of the pores induced by the foaming process. In fact, for both PCL/TZ and PCL/TZ-HA samples we observed the preferential pore formation into the PCL phase, while an almost non-porous TZ morphology was obtained (Fig. 1). This effect is mainly ascribable to the specific saturation and foaming temperatures selected, lower than the glass transition temperature of the TZ (50 °C) [12], which did not allow enough TZ plasticization. As a direct consequence, TZ foaming was impaired by the low $scCO_2$ solubilization and, by the high rigidity of the TZ/$scCO_2$ solution (black arrows of Fig. 1). These results were in agreement with those of a previously reported work on similar multi-phase systems obtained by blending PCL and thermoplastic gelatin [21]. As shown in Fig. 1, $scCO_2$ is, conversely able to significantly plasticize PCL, as also reported in other works [8,20], therefore allowing for the foaming of the PCL phase of the multi-phase systems (white arrows of Fig. 1). Nevertheless, the presence of the TZ network surrounding the expandable PCL domains, conceivably decreased the foamability of PCL and, consequently, did not allow for the formation of a macro-porosity of the order of hundreds of microns required for the proposed application. In fact, the presence of TZ restricted pore sizes to tens of microns. This effect also explained the rather low increase of the pore size observed after the increase of the depressurization time from 15 to 120 s (Fig. 1c and d), as it has been generally observed than an increase of the depressurization time, resulted in higher pores formation [8,11]. The higher magnification of the SEM micrograph reported in Fig. 1c also showed that the increase of the depressurization time from 15 to 120 s was responsible for the formation of tiny small pores within the TZ.

By comparing the left and right SEM micrographs of Fig. 1, we may clearly observe the presence of the HA particles within the polymeric matrix of the composite foams, while minor differences were observed on the pore structure of the foams as a function of the HA incorporation. Although it is well known that the incorporation of inorganic particles within a polymer may affect its foaming behavior [22], the observed effect may be explained by considering the multi-phase nature of our system and, the different foaming behavior of the two polymers. Indeed, the higher chemical affinity of the HA particles to the TZ, if compared to PCL, may allow for their preferential distribution within the TZ domains (Fig. 1). This effect, in addition to the limited foaming behavior of PCL and TZ, resulted in minor differences on the pore structure between PCL/TZ and PCL/TZ-HA foamed samples.

Taking into the account all of these results and, by considering the need to induce the formation of larger pores within the PCL/TZ and PCL/TZ-HA samples, we performed further foaming experiments by processing the biomaterials at higher temperatures. In particular, $scCO_2$ solubilization was carried out at 80 °C

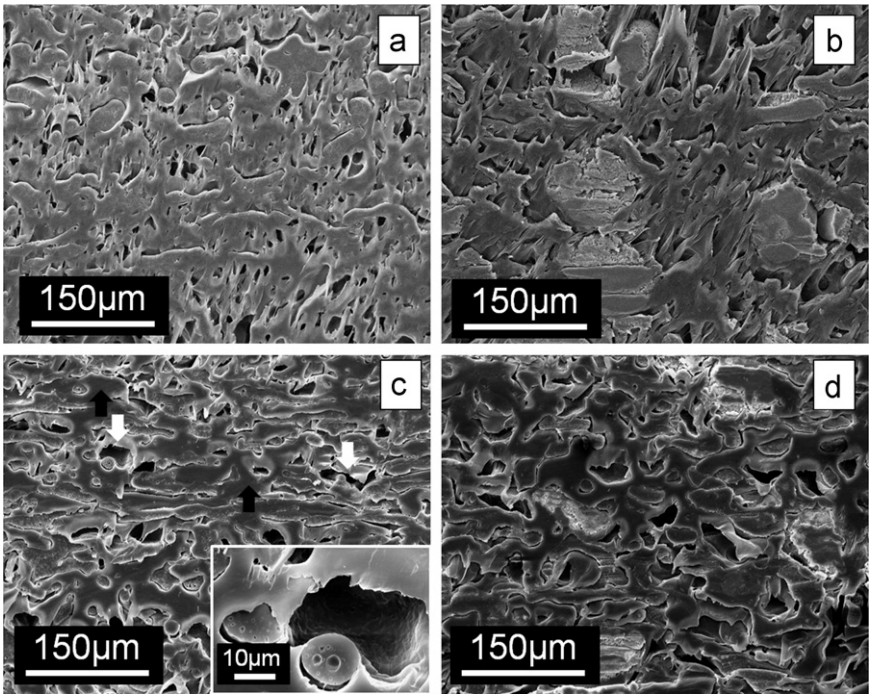

Fig. 1. SEM micrographs of the PCL/TZ (a and c) and PCL/TZ-HA (b and d) foamed samples prepared *via* the solid-state $scCO_2$ foaming and by using a depressurization time of 2 s (a and b) and 120 s (c and d). Black and white arrows indicated the foamed TZ and PCL phases, respectively.

and 9 MPa for 4 h. These conditions were suitable to allow for a sufficient solubilization of the blowing agent within both PCL and TZ [6,23]. After solubilization, the temperature of the system was then increased up to 110 °C and, the pressure quenched to the ambient by a depressurization time of 15 s.

The results of the morphological characterization of the obtained samples are reported in Fig. 2. As shown, the foaming process induced the formation of porous samples with bi-modal pore size distributions. In particular, a macro-porosity was obtained in the PCL phase as a consequence of the foaming and subsequent collapse of the pores at the interface with the TZ (large pores in Fig. 2a and b). Indeed, at the foaming temperature selected, PCL was unable to crystallize and stabilize the pore structure and, consequently, collapsed at the interface with the surrounding TZ network [21]. As a result, an elongated macro-pore was formed within each PCL domain of the starting co-continuous blend. With respect to the TZ, the selection of processing temperatures (saturation and foaming) higher than its glass transition temperature, enhanced the TZ plasticization and subsequent foaming. Nevertheless, differently from the macro-porosity of the PCL phase, for which we observed the presence of pore interconnections, dictated by the co-continuity of the blend, the porosity generated within the TZ phase evidenced an almost closed-morphology (Fig. 2). To overcome this limitation and, to improve the interconnectivity of the bi-modal scaffolds, we extracted the plasticizer from TZ by soaking the samples in water at 37 °C overnight. Indeed, zein is a vegetal protein characterized by a high portion of hydrophobic amino acids and, therefore, evidences slow dissolution in water [16]. Conversely, PEG is highly soluble in water. The efficacy of this process was verified first by testing non porous TZ samples. Fig. 3 shows SEM micrographs of the resulting TZ sample, clearly showing the presence of a uniform distribution of small pores. These pores are substantially generated by the dissolution of the PEG-rich fractions from the TZ, leading to the formation of an open porous zein matrix. Furthermore, the hydrophilic nature of zein and its accelerated degradation, if compared to PCL, may ensure the fast increase of micro-pore throat and interconnectivity.

Based on these results, we implemented the same process on the multi-phase foamed samples prepared at temperatures higher than PCL melting and, the results of the morphological and microstructural characterizations were reported in the following section.

3.2. Morphology and micro-structural properties of the bi-modal PCL/TZ and PCL/TZ-HA scaffolds

Fig. 4 reported the morphology of the scaffolds obtained by combining $scCO_2$ foaming and PEG leaching processes. As shown in Fig. 4a–d, the scaffolds were characterized by a bi-modal pore structure. In particular, the macro-porosity obtained during the foaming step was homogeneously distributed within a micro-porous TZ network. Furthermore, differently from the morphology of the foamed samples before the leaching process, reported in Fig. 2, in this case we observed that the pore structure of the TZ network was characterized by a micro-porosity similar to that of neat TZ (compare Figs. 3d and 4e). By considering the co-continuous nature of the initial blend, this result confirmed the possibility of extracting the PEG from the TZ phase of the foamed samples, allowing for the fabrication of PCL/TZ and PCL/TZ-HA porous scaffolds with bi-modal pore size distribution and more interconnected micro-porosity. The high magnification SEM micrograph of Fig. 4f evidenced the porosity of the HA granules dispersed within the composite scaffold. This nano-porous structure may enhance the biological response of the scaffold by providing a biomimetic structure able to stimulate bone cell spreading and differentiation [24].

The results of the porosity measurements of the scaffolds are reported in Table 1. As shown, the overall porosity decreased from 68.47 ± 2.71 to $62.9 \pm 3.43\%$ with the incorporation of the HA particles within the polymeric matrix ($p < 0.05$). These results are in agreement with those of the morphological characterization (Fig. 4) and, also, with literature studies demonstrating the decrease of the expansion ratio of polymeric foams prepared *via* $scCO_2$ foaming after the incorporation of inorganic fillers [22]. It is also important to point out that, although higher porosity values, up to 95%, may enhance cell colonization and infiltration, the presence of zein is

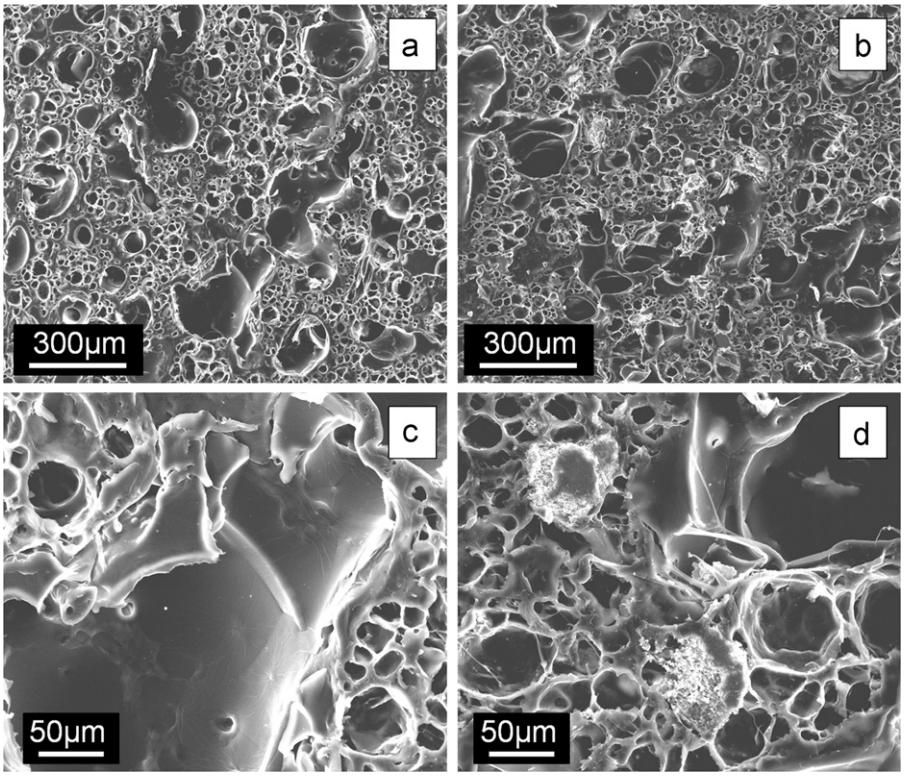

Fig. 2. SEM micrographs of the PCL/TZ (a and c) and PCL/TZ-HA (b and d) foamed samples prepared at saturation temperature and pressure equal to 80 °C and 9 MPa, respectively and, by performing foaming at 110 °C.

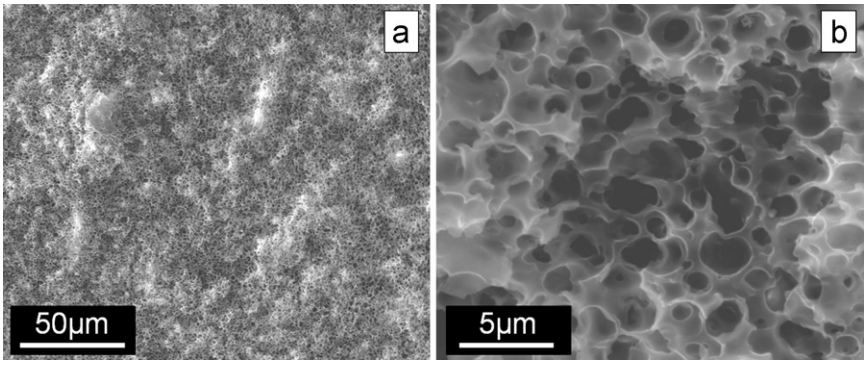

Fig. 3. SEM micrographs of the TZ after the selective extraction of the plasticizer performed by soaking the sample in water at 37 °C overnight.

expected to accelerate scaffold degradation [12] and increase its porosity. Concomitantly, the PCL may guaranty the structural support until the new forming tissue can assume its own structural role.

The pore size distributions of the scaffolds were reported in Fig. 5. According to the previous results, the PCL/TZ and PCL/TZ-HA scaffolds were characterized by a bi-modal pore size distribution. In particular, the scaffolds evidenced a micro-porosity in the 1–10 μm range, coupled with a macro-porosity in the 20–400 μm range.

Table 1
Porosity and mechanical compression properties of the bi-modal PCL/TZ and PCL/TZ-HA composite scaffolds prepared by the $scCO_2$ foaming and porogen leaching combined process.

Sample	Porosity (%)	E (MPa)	ε_Y (mm/mm)	σ_Y (MPa)
PCL/TZ	68.47 ± 2.71	17.80 ± 3.45	0.18 ± 0.05	2.60 ± 0.36
PCL/TZ-HA	62.9 ± 3.43	38.30 ± 7.70	0.12 ± 0.03	3.67 ± 0.15

Furthermore, the mean pore size of the micro-porosity, equal to 3 μm, was not affected by the composition of the starting materials. Conversely, the mean pore size of the macro-porosity decreased slightly from 134 ± 80 μm for the PCL/TZ to 121 ± 49 μm for the PCL/TZ-HA scaffolds, indicating the decrease of the expansion ratio of the samples after the incorporation of the HA particles. Although this difference was not found to be statistically significant, the decrease of the size of the macro-pores is ascribable to the decrease of the size of the PCL domains and to the increase of the stiffness of the polymeric matrix as a consequence of the incorporation of the HA particles. As expected, a mono-modal pore size distribution with mean pore size equals to 3 μm was observed for neat TZ sample.

Providing an adequate mechanical support is a critical bTE scaffold design requirement. Indeed, in the case of load-bearing tissues, such as bone, the porous scaffold must provide a temporary substrate for cell adhesion, growth and proliferation, coupled with the capability to withstand *in vivo* stresses and loading and to avoid

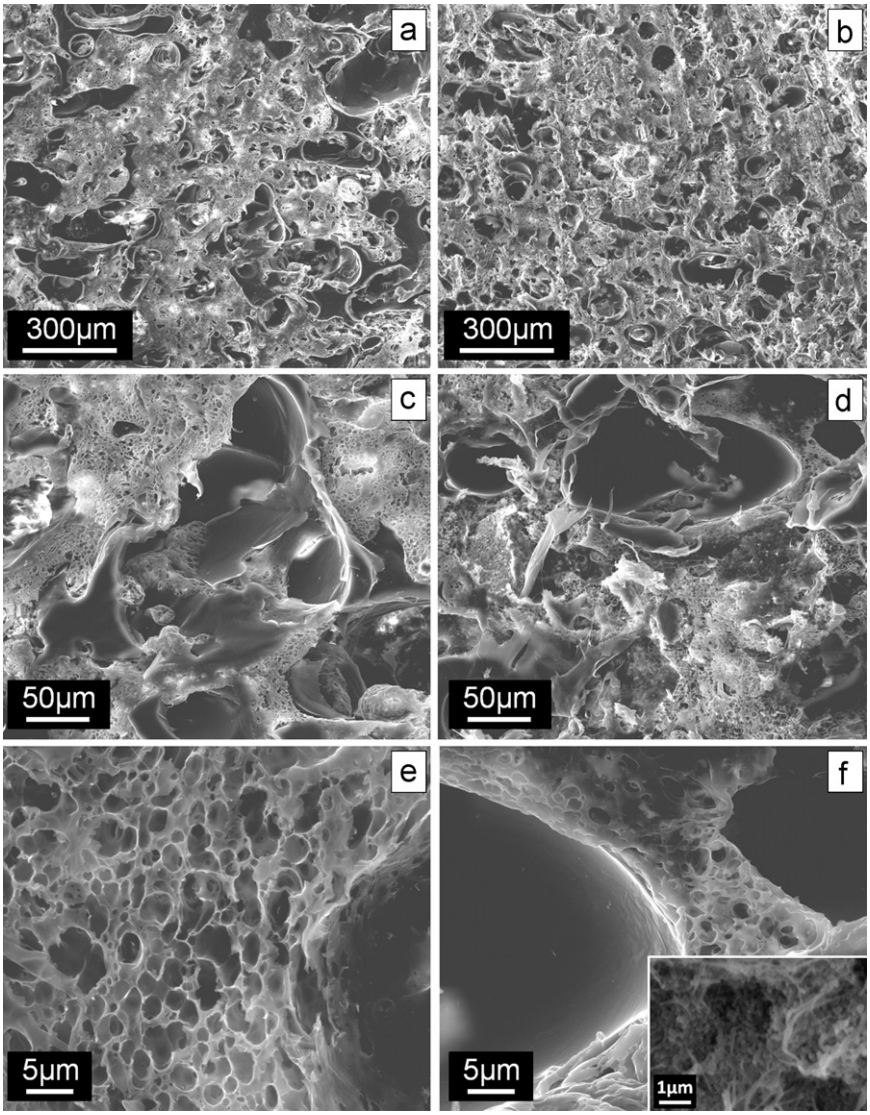

Fig. 4. SEM micrographs of the bi-modal PCL/TZ (a, c and e) and PCL/TZ-HA (b, d and f) scaffolds prepared by the $scCO_2$ foaming and porogen leaching combined process. The inset in (f) evidences the nano-porosity of the HA granule of the PLC/TZ-HA composite scaffold.

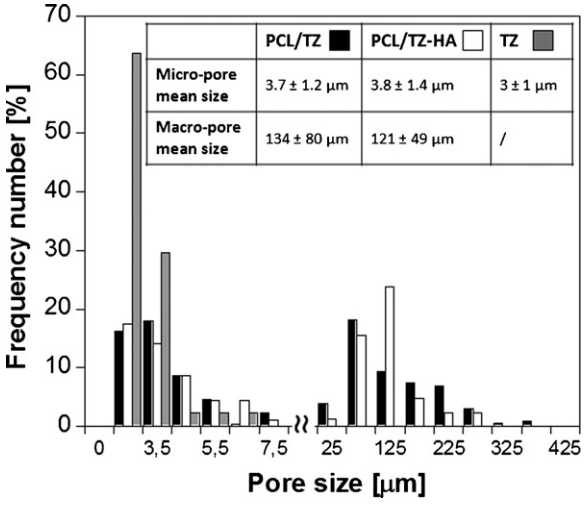

Fig. 5. Pore size distribution of the bi-modal PCL/TZ and PCL/TZ-HA composite scaffolds. The pore size distribution of the TZ after the leaching of the plasticizer is also reported for comparison.

excessive new-tissue deformation [25]. The scaffolds prepared in this study showed the typical σ–ε curve of porous materials undergoing static compression testing (data not shown). In particular, the initial linear-elastic region was followed by a short collapse plateau and, finally, the steep increase in the stress values caused by the densification phenomenon was observed [6,23]. As reported in Table 1, the calculated average values of E were 17.8 ± 3.45 and 38.3 ± 7.7 MPa for the PCL/TZ and PCL/TZ-HA scaffold, respectively.

Literature studies indicated that, scaffolds for bTE must possess a value of E equal or higher than 10 MPa, as those of the scaffolds prepared in this study [25]. The increased stiffness observed in the case of the PCL/TZ-HA scaffold was also confirmed by the decrease of ε_Y from 0.18 ± 0.05 to 0.12 ± 0.03 mm/mm and by the increase of σ_Y from 2.6 ± 0.36 to 3.7 ± 0.15 MPa after the incorporation of the HA particles within the polymeric matrix. These effects were ascribable to several factors, such as the decrease of the overall porosity of the scaffolds after the incorporation of the HA particles (Table 1), as well as the presence of a macro-porosity characterized by smaller pores and a narrower pore size distribution (Fig. 5). Furthermore, the HA particles also acted as a reinforcing filler for the polymeric matrix and, consequently, increased the capability of the porous scaffold to respond to the external compression load [26].

3.3. In vitro cell/scaffold interaction

In characterizing the biocompatibility of porous scaffolds for bTE, the selection of cells source and culture conditions are critical parameters, because they may extensively influence seeded population behavior and, the eventual structure and properties of the engineered tissue [27,28]. The biocompatibility of the bi-modal PCL/TZ and PCL/TZ-HA composite scaffolds was assessed *in vitro* by using pre-osteoblasts MG63 cells. These cells are at a relatively early state in the osteoblastic lineage and, consequently, may represent a good model to investigate the biological response of the scaffolds [27,28].

Alamar Blue assay was performed in order to evaluate cell viability and proliferation and the results are reported in Fig. 6. As shown, the scaffolds supported cell proliferation up to 28 days of *in vitro* culture. In particular, for the PCL/TZ scaffold, the number of viable cells increased from $7.6 \pm 0.4 \times 10^3$ at day 7 to $26.7 \pm 0.1 \times 10^3$ at day 28 ($p < 0.05$). A slight higher number of viable cells was observed in the case of the PCL/TZ-HA composite scaffold at each time points of culture, demonstrating also the positive effect exerted by the HA particles on the biological response of the scaffolds. Standard culture plates were used as control for cell proliferation, showing a higher cell adhesion and proliferation in the whole culture period (Fig. 6).

The ability of the scaffolds to support the adhesion, colonization and proliferation of the MG63 cells was confirmed by the SEM analysis of the seeding surface of the cell/scaffold constructs over culture time, reported in Figs. 7 and 8. At 7 days of *in vitro* culture, the MG63 colonized the surface of the scaffold, preferentially adhering within the macro-porosity obtained by the foaming process (arrows in the SEM micrographs reported in Fig. 7c and d). Furthermore, the morphological characterization also showed that the cells were characterized by a flat morphology and entered within the interior of the pore structure by the creation of bridges between opposite pore walls. After 28 days of *in vitro* culture, we observed the formation of cell layers within the macro-porosity of the scaffolds, making it difficult to distinguish the supporting scaffold pore structure (Fig. 8c and d).

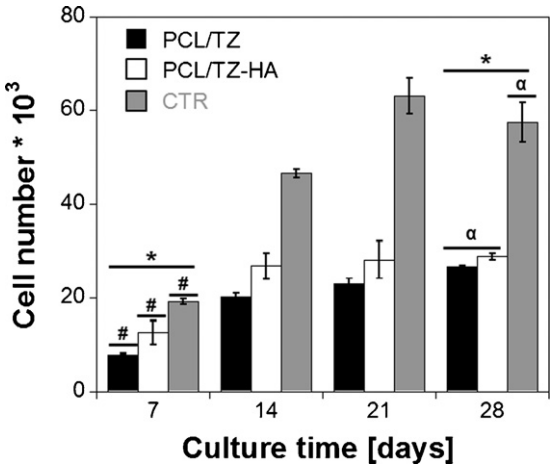

Fig. 6. Cell proliferation on the bi-modal PCL/TZ and PCL/TZ-HA composite scaffolds as evaluated by the Alamar Blue test ($n = 5$). Standard 2D-cultures on tissue culture plates (TCPS) are also shown as control.

Cell adhesion, proliferation and colonization within porous three-dimensional scaffolds are interdependent events guided by parameters such as scaffold's material chemistry and pore structure features, among others [5,6,17]. From the scaffold materials point of view, our results confirmed those reported in literature about the biocompatibility of PCL, zein and HA [1,3,6,15–17]. For instance, recent studies proved that zein can reduce blood pressure in hypertensive rats, and may be used for liver and fibroblast cells culture [16]. Furthermore, porous zein scaffolds and its composites with HA were found to support *in vitro* MSCs adhesion, proliferation and osteogenic differentiation and, *in vivo* bone formation [17,18]. We

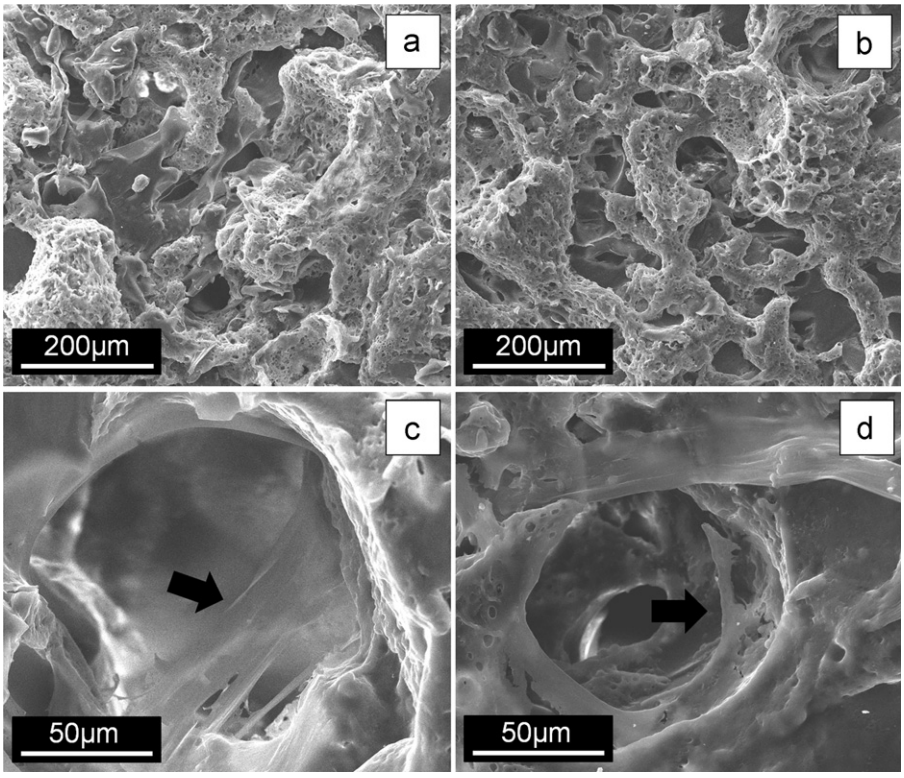

Fig. 7. SEM micrographs of the seeding surface of the cell/scaffold constructs after 7 days of *in vitro* culture: (a and c) PCL/TZ and (b and d) PCL/TZ-HA composite scaffolds.

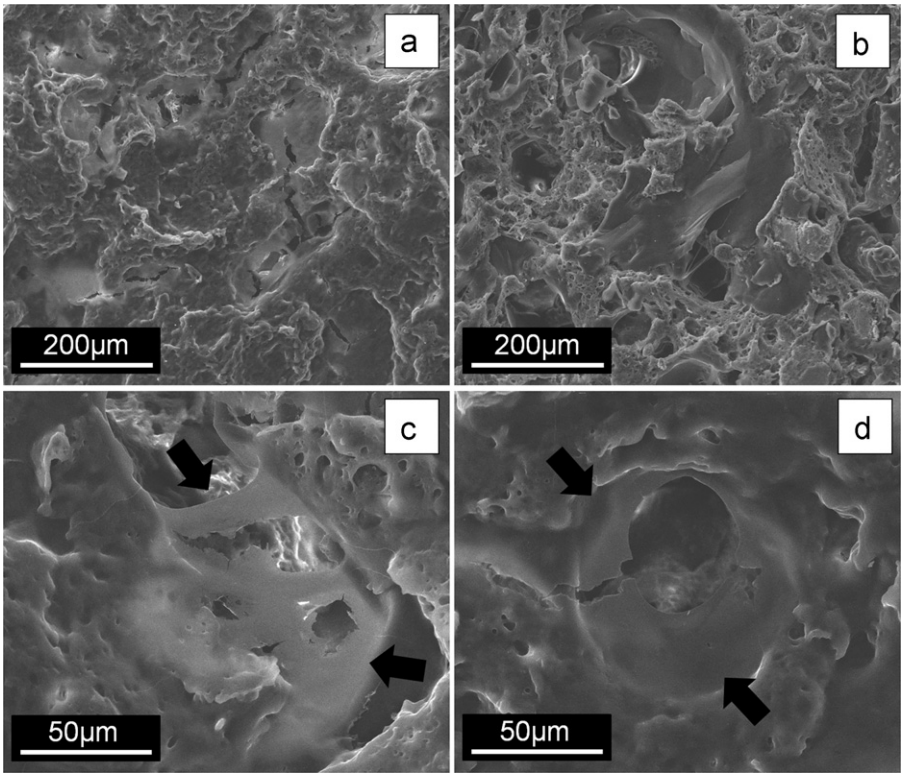

Fig. 8. SEM micrographs of the seeding surface of the cell/scaffold constructs after 28 days of *in vitro* culture: (a and c) PCL/TZ and (b and d) PCL/TZ-HA composite scaffolds.

have recently characterized the *in vitro* biological response of non-porous multi-phase PCL/TZ and PCL/TZ-HA composite biomaterials by using mesenchymal stem cells and MG63 cells [12,13]. The results of these studies demonstrated that the proposed materials were able to support cell adhesion, proliferation and differentiation [12,13]. Based on these findings, in this study we developed a combined process for the preparation of bi-modal porous PCL/TZ and PCL/TZ-HA scaffolds with micro-structural features suitable for bTE and, we characterized their ability to be used as scaffolds for osteoblast culture. The biological characterization confirmed the results achieved in our previous studies and, additionally, demonstrated the importance of the architecture of the pore structure of the scaffolds on osteoblasts growth and proliferation *in vitro*.

As previously discussed, the pore structure plays a fundamental role for the success of any tissue engineering scaffold-based approach. For instance, it has been demonstrated that different tissues require different pore sizes for their regeneration and, that the diameter of cells in suspension dictates the minimum pore size, which varies from one cell type to another [3,4]. As clearly showed in this study, cell adhesion, colonization and proliferation occurred preferentially within the macro-porosity of the scaffolds (Figs. 7 and 8). This result was in agreement with literature studies indicating that a macro-porosity in the range from 100 to 400 μm provides the optimal pore size for osteoblasts ingrowths [1,3,4]. The presence of the macro-porosity also ensures an adequate substrate for cell growth and proliferation, as demonstrated by the Alamar Blue results of Fig. 6 and, by the morphological results of Figs. 7 and 8. It is however important to point out that the pore structure acted in synergy with the composition of the scaffolds, as demonstrated by the increased MG63 proliferation when cultured on the multi-phase PCL/TZ-HA composite scaffold, if compared to the PCL/TZ one. Similar results were reported by Yoshida et al. for MG63 cultured within porous hydroxyapatite/collagen nanocomposite scaffolds [29], finally indicating that the multi-phase composite scaffold produced by combining PCL, TZ and HA may be a good candidate for bTE purposes.

4. Conclusions

This study reported the design and fabrication of bi-modal porous scaffolds for bTE by using a completely green process based on the combination of the techniques of $scCO_2$ foaming and porogen leaching.

By this approach we fabricated porous PCL/TZ and PCL/TZ-HA scaffolds characterized by double scale pore size distributions with a macro-porosity of mean pore size of 134 ± 80 μm and 121 ± 49 μm, respectively, and a micro-porosity in the 1–10 μm range. Furthermore, the scaffolds evidenced porosity values equal to $68.47 \pm 2.71\%$ and $62.90 \pm 3.43\%$ and static compression moduli equal to $17.80 \pm 3.45\%$ and 38.30 ± 7.70 MPa, respectively. Finally, the results of the *in vitro* biological tests demonstrated the ability of the scaffolds to support and promote the adhesion, colonization and proliferation of osteoblast cells, as evidenced by the increase of the number of viable cells from $7.6 \pm 0.4 \times 10^3$ at day 7 to $26.7 \pm 0.1 \times 10^3$ at day 28 for the PCL/TZ scaffold and from $12.6 \pm 2.5 \times 10^3$ at day 7 to $28.8 \pm 0.7 \times 10^3$ at day 28 for the PCL/TZ-HA scaffold.

Acknowledgments

The authors thank Domenico De Gennaro for his support to carry out the experimental activity. This research has been supported by a grant from the Italian Ministry of Health, TISSUENET n. RBPR05RSM2.

References

[1] D.W. Hutmacher, Scaffolds in tissue engineering bone and cartilage, Biomaterials 21 (2000) 2529–2543.
[2] J.R. Porter, T.T. Ruckh, K.C. Popat, Bone tissue engineering: a review in bone biomimetics and drug delivery strategies, Biotechnology Progress 25 (2009) 1539–1560.
[3] S. Yang, K. Leong, Z. Du, C. Chua, The design of scaffolds for use in tissue engineering. Part I. Traditional factors, Tissue Engineering 7 (2001) 679–689.
[4] V. Guarino, F. Causa, A. Salerno, L. Ambrosio, P.A. Netti, Design and manufacture of microporous polymeric materials with hierarchal complex structure for biomedical application, Materials Science & Technology 24 (2008) 1111–1117.
[5] M.M.C.G. Silva, L.A. Cyster, J.J.A. Barry, X.B. Yang, R.O.C. Oreffo, D.M. Grant, C.A. Scotchford, S.M. Howdle, K.M. Shakesheff, F.R.A. Rose, The effect of anisotropic architecture on cell and tissue infiltration into tissue engineering scaffolds, Biomaterials 35 (2006) 5909–5917.
[6] A. Salerno, D. Guarnieri, M. Iannone, S. Zeppetelli, P.A. Netti, Effect of micro- and macroporosity of bone tissue three-dimensional-poly(e-caprolactone) scaffold on human mesenchymal stem cells invasion, proliferation, and differentiation in vitro, Tissue Engineering: Part A 16 (2010) 2661–2673.
[7] D.L. Elbert, Bottom-up tissue engineering, Current Opinion in Biotechnology 22 (2011) 674–680.
[8] A. Salerno, S. Zeppetelli, E. Di Maio, S. Iannace, P.A. Netti, Design of bimodal PCL and PCL-HA nanocomposite scaffolds by two step depressurization during solid-state supercritical CO_2 foaming, Macromolecular Rapid Communications 32 (2011) 1150–1156.
[9] V.E. Santo, A.R.C. Duarte, M.E. Gomes, J.F. Mano, R.L. Reis, Hybrid 3D structure of poly(D,L-lactic acid) loaded with chitosan/chondroitin sulfate nanoparticles to be used as carriers for biomacromolecules in tissue engineering, J. Supercritical Fluids 54 (2010) 320–327.
[10] P.J. Ginty, D. Howard, C.E. Upton, J.J.A. Barry, F.R.A.J. Rose, K.M. Shakesheff, S.M. Howdle, A supercritical CO_2 injection system for the production of polymer/mammalian cell composites, J. Supercritical Fluids 43 (2008) 535–541.
[11] E. Kiran, Foaming strategies for bioabsorbable polymers in supercritical fluid mixtures. Part II. Foaming of poly(ε-caprolactone-co-lactide) in carbon dioxide and carbon dioxide + acetone fluid mixtures and formation of tubular foams via solution extrusion, J. Supercritical Fluids 54 (2010) 308–319.
[12] A. Salerno, M. Oliviero, E. Di Maio, P.A. Netti, C. Rofani, A. Colosimo, V. Guida, B. Dallapiccola, P. Palma, E. Procaccini, A.C. Berardi, F. Velardi, A. Teti, S. Iannace, Design of novel three-phase PCL/TZ-HA biomaterials for use in bone regeneration applications, J. Materials Science Materials in Medicine 21 (2010) 2569–2581.
[13] A. Salerno, S. Zeppetelli, M. Oliviero, E. Battista, E. Di Maio, S. Iannace, P.A. Netti, Micro-structure, degradation and in vitro MG63 cells interaction with a novel biodegradable composite made of poly(ε-caprolactone), thermoplastic zein and hydroxyapatite for bone tissue engineering, J. Bioactive and Compatible Polymers (2012), in press, http://dx.doi.org/10.1177/0883911512442564.
[14] R. Murugan, S. Ramakrishna, Development of nanocomposites for bone grafting, Composites Science and Technology 65 (2005) 2385–2406.
[15] A.R. Boccaccini, M. Erol, W.J. Stark, D. Mohn, Z. Hong, J.F. Mano, Polymer/bioactive glass nanocomposites for biomedical applications: a review, Composites Science and Technology 70 (2010) 1764–1776.
[16] J. Dong, Q. Sun, J. Wang, Basic study of corn protein, zein, as a biomaterial in tissue engineering, surface morphology and biocompatibility, Biomaterials 25 (2004) 4691–4697.
[17] Z. Qu, H. Wang, T. Tang, X. Zhang, J. Wang, K. Dai, Evaluation of the zein/inorganics composite on biocompatibility and osteoblastic differentiation, Acta Biomaterialia 4 (2008) 1360–1368.
[18] J. Tu, H. Wang, H. Li, K. Dai, J. Wang, X. Zhang, The in vivo bone formation by mesenchymal stem cells in zein scaffolds, Biomaterials 30 (2009) 4369–4376.
[19] R.B. Yoganathana, R. Mammucari, N.R. Foster, Dense gas processing of polymers, Polymer Reviews 50 (2010) 144–177.
[20] Z. Lian, S.A. Epstein, C.W. Blenk, A.D. Shine, Carbon dioxide-induced melting point depression of biodegradable semicrystalline polymers, J. Supercritical Fluids 39 (2006) 107–117.
[21] A. Salerno, M. Oliviero, E. Di Maio, S. Iannace, P.A. Netti, Design and preparation of μ-bimodal porous scaffold for tissue engineering, J. Applied Polymer Science 106 (2007) 3335–3342.
[22] N.J. Collins, R.H. Bridson, G.A. Leeke, L.M. Grover, Particle seeding enhances interconnectivity in polymeric scaffolds foamed using supercritical CO_2, Acta Biomaterialia 6 (2010) 1055–1060.
[23] A. Salerno, M. Oliviero, E. Di Maio, S. Iannace, Thermoplastic foams from gelatin and zein, International Polymer Processing 5 (2007) 1–9.
[24] I. Gerçek Beşkardeş, M. Gümüşderelioğlu, Biomimetic apatite-coated PCL scaffolds: effect of surface nanotopography on cellular functions, J. Bioactive and Compatible Polymers 24 (2009) 507.
[25] S.J. Hollister, Porous scaffold design for tissue engineering, Nature Materials 4 (2005) 518–524.
[26] C.R. Kothapalli, M.T. Shaw, M. Wei, Biodegradable HA-PLA 3D porous scaffolds: Effect of nano-sized filled content on scaffold properties, Acta Biomaterialia 1 (2005) 653–662.
[27] J.C. Meredith, J. Sormana, B.G. Keselowsky, A.J. García, A. Tona, A. Karim, E.J. Amis, Combinatorial characterization of cell interactions with polymer surfaces, J. Biomedical Materials Research 66A (2003) 483–490.
[28] T.P. Kunzler, T. Drobek, M. Schuler, N.D. Spencer, Systematic study of osteoblast and fibroblast response to roughness by means of surface-morphology gradients, Biomaterials 13 (2007) 2175–2182.
[29] T. Yoshida, Y. Koyama, M. Kikuchi, K. Takakuda, Osteogenic activity of MG63 cells on bone-like hydroxyapatite/collagen nanocomposite sponges, J. Materials Science Materials in Medicine 21 (2010) 1263–1272.